SUPPORTING INFORMATION for:

A Solid-State ^{11}B NMR and Computational Study of Boron Electric Field Gradient and Chemical Shift Tensors in Boronic Acids and Boronic Esters

Joseph W. E. Weiss and David L. Bryce*

Department of Chemistry and Centre for Catalysis Research and Innovation

University of Ottawa

Ottawa, Ontario K1N 6N5, Canada

* Author to whom correspondence should be addressed.

phone: 1-613-562-5800 ext 2018

fax: 1-613-562-5170

email: dbryce@uottawa.ca

Table S1. Calculated ^{11}B EFG parameters and CSA for compounds **1** to **10**.[a]

		B3LYP			RHF			GGA revPBE			
	Sample	C_Q / MHz	η_Q	Ω / ppm	C_Q / MHz	η_Q	Ω / ppm	C_Q / MHz	η_Q	Ω / ppm	ϕ_{CCBO} / °
Boronic Acids	1	2.82	0.631	17.1	2.84	0.614	16.6	2.83	0.644	21.9	0.0
	1†	2.61	0.494	22.0	3.09	0.419	20.1	2.81	0.570	25.0	8.7
	2	2.92	0.439	36.0	2.90	0.422	34.7	2.96	0.383	43.7	90.0
	2†	2.86	0.302	38.4	2.88	0.288	38.0	2.91	0.380	41.8	90.0
	3	2.23	0.922	16.6	2.42	0.782	17.0	2.81	0.504	33.4	28.1
	3†	2.80	0.338	22.7	2.79	0.339	22.4	2.74	0.362	27.7	0.1
	4	2.78	0.466	13.8	3.34	0.364	10.3	2.68	0.447	18.7	0.0
	4†	2.76	0.561	22.4	3.32	0.426	18.7	2.68	0.553	23.4	0.0
	5	2.07	0.548	15.8	2.11	0.377	17.2	2.84	0.524	32.6	36.7
	5†	2.43	0.449	24.7	2.43	0.449	24.8	2.68	0.537	28.1	19.9
Boronic Esters	6	2.72	0.621	17.0	2.72	0.624	16.0	2.62	0.649	23.9	0.5
	7	2.78	0.582	11.5	2.79	0.574	10.8	2.72	0.545	11.5	3.0
	8	2.79	0.640	15.5	2.80	0.638	15.4	2.71	0.632	15.5	2.9
	9	2.62	0.677	12.0	3.09	0.586	17.6	2.73	0.592	14.0	1.2
	10	2.10	0.186	15.5	2.14	0.274	16.7	2.74	0.529	32.3	61.3
Boric Acid		2.30	0.249	10.7	2.90	0.183	7.9	2.24	0.300	11.4	0.0

†Corresponds to boronic acid dimer

[a] Calculated boron C_Q, η_Q, and Ω values for each boronic acid and ester compound studied. Calculated values for boronic acid dimers which take into account hydrogen bonding interactions are included where applicable. Hybrid DFT calculations were performed using the B3LYP functional and the 6-31G* basis set on all first and second row elements, while the aug-cc-pVTZ basis set was used on all heavier elements. RHF calculations were performed using the 6-31G* basis set on all first and second row elements, while the aug-cc-pVTZ basis set was used on all heavier elements. ADF calculations were performed using the GGA revPBE functional and TZP basis set on all atoms. ϕ_{CCBO} is shown (see Figure 18). Boric acid is included as the impurity present at 19.6 ppm in compounds **2** and **3**.

Table S2. Calculated magnetic shielding tensor skew and Euler angles for compounds **1** to **10** using two different basis sets.[a]

		B3LYP				RHF			
	Sample	κ	α	β	γ	κ	α	β	γ
Boronic Acids	1	0.79	295	0	82	0.78	283	0	98
	1†	-0.19	136	16	246	-0.60	300	16	71
	2	0.47	236	0	214	0.36	180	0	270
	2†	0.15	2	0	143	0.09	353	0	151
	3	0.54	357	14	77	0.43	355	15	78
	3†	-0.50	319	0	169	-0.48	314	0	173
	4	-0.96	24	0	90	-0.81	217	90	270
	4†	-0.27	306	90	90	-0.12	121	90	270
	5	0.85	2	18	69	0.85	2	17	74
	5†	-0.35	133	19	254	-0.34	133	18	253
Boronic Esters	6	0.63	270	1	180	0.67	90	1	360
	7	0.00	359	0	1	-0.29	0	2	360
	8	-0.84	77	0	282	-0.96	268	89	91
	9	-0.45	164	2	197	-0.58	91	90	268
	10	0.84	184	9	175	0.86	5	9	354
Boric Acid		-0.68	151	0	203	-0.78	84	90	270

†Corresponds to boronic acid dimer

[a] Calculated boron Euler angles, which represent the corresponding angles between the EFG and shielding tensor components in their respective PASs, and κ values for each boronic acid and ester compound studied. Calculated values for boronic acid dimers which take into account hydrogen bonding interactions are included where applicable. Hybrid DFT calculations were performed using the B3LYP functional and the 6-31G* basis set on all first and second row elements, while the aug-cc-pVTZ basis set was used on all heavier elements. RHF calculations were performed using the 6-31G* basis set on all first and second row elements, while the aug-cc-pVTZ basis set was used on all heavier elements. ADF calculations were performed using the GGA revPBE functional and TZP basis set on all atoms. Boric acid is included as the impurity present at 19.6 ppm in compounds **2** and **3**.

Table S3. Calculated magnetic shielding tensor skew and Euler angles for compounds **1** to **10** using a single basis set on all atoms.[a]

		B3LYP				RHF			
	Sample	κ	α	β	γ	κ	α	β	γ
Boronic Acids	1	0.81	6	0	11	0.15	276	0	90
	1†	0.24	182	8	201	0.05	242	7	62
	2	0.44	223	0	227	0.69	178	0	272
	2†	0.0	326	0	187	0.22	87	0	68
	3	0.24	356	6	76	0.37	41	0	89
	3†	-0.24	156	0	254	0.01	154	0	249
	4	-0.87	200	0	276	-0.76	217	90	270
	4†	-0.38	127	90	270	-0.14	209	90	90
	5	0.64	177	16	275	0.73	175	13	294
	5†	-0.36	131	12	253	-0.15	219	13	306
Boronic Esters	6	0.71	90	1	0	0.44	90	3	90
	7	0.23	0	1	360	-0.93	0	1	360
	8	-0.58	30	1	329	-0.57	268	90	90
	9	-0.20	111	1	251	-0.79	91	88	269
	10	0.88	342	5	66	0.44	347	8	12
Boric Acid		-0.69	241	0	112	-0.67	264	90	90

†Corresponds to boronic acid dimer

[a] Calculated boron κ and Euler angles for each boronic acid and ester compound studied. Calculated values for boronic acid dimers which take into account hydrogen bonding interactions are included where applicable. Hybrid DFT calculations were performed using the B3LYP functional and the 6-311+G* basis set on all elements. RHF calculations were performed using the 6-311+G* basis set on elements. ADF calculations were performed using the GGA revPBE functional and TZP basis set on all atoms. Boric acid is included as the impurity present at 19.6 ppm in compounds **2** and **3**.

Table S4. Calculated magnetic shielding tensor components for compounds **1** to **10**.[a]

Boronic Acids	**1**				**2**				**3**				**4**				**5**			
Contribution	σ_{11}	σ_{22}	σ_{33}	σ_{iso}	σ_{11}	σ_{22}	σ_{33}	σ_{iso}	σ_{11}	σ_{22}	σ_{33}	σ_{iso}	σ_{11}	σ_{22}	σ_{33}	σ_{iso}	σ_{11}	σ_{22}	σ_{33}	σ_{iso}
σ^d (Core Density)	163.9	164.1	164.3	164.1	163.4	164.2	164.7	164.1	163.8	164.2	164.4	164.1	163.8	164.2	164.3	164.1	163.8	164.1	164.4	164.1
σ^d (Valence Density)	-0.5	33.6	38.3	23.8	8.5	29.5	34.5	24.2	-0.5	32.8	39.1	23.8	4.2	32.9	40.9	24.6	3.1	34.2	39.6	25.6
σ^d	163.4	197.7	202.6	187.9	171.9	193.7	199.2	188.3	163.3	197.0	203.5	187.9	168.0	197.1	205.2	188.7	166.9	198.3	204.0	189.8
σ^p (OCC-OCC)	22.9	28.6	162.0	71.2	16.4	62.2	101.6	60.1	10.8	21.0	132.9	54.9	12.3	22.6	138.4	57.8	14.5	19.4	123.7	52.5
σ^p (OCC-VIR)	-307.6	-177.8	-156.6	-214.0	-273.5	-157.0	-138.2	-189.6	-251.8	-161.9	-138.7	-184.1	-267.3	-163.6	-143.8	-191.5	-248.7	-157.9	-143.7	-183.4
σ^p	-142.0	-128.7	-81.3	-117.4	-143.6	-125.9	-80.0	-116.5	-141.1	-127.6	-79.4	-116.1	-142.3	-125.8	-94.0	-120.7	-141.8	-127.9	-82.4	-117.4
Total	57.5	71.6	82.5	70.6	51.4	70.8	93.2	71.8	56.2	75.6	83.8	71.9	55.4	69.8	78.8	68.0	57.2	74.5	85.3	72.4

*Boronic acid calculations are performed on the dimer

Boronic Esters	**6**				**7**				**8**				**9**				**10**			
Contribution	σ_{11}	σ_{22}	σ_{33}	σ_{iso}	σ_{11}	σ_{22}	σ_{33}	σ_{iso}	σ_{11}	σ_{22}	σ_{33}	σ_{iso}	σ_{11}	σ_{22}	σ_{33}	σ_{iso}	σ_{11}	σ_{22}	σ_{33}	σ_{iso}
σ^d (Core Density)	163.8	164.1	164.4	164.1	163.8	164.1	164.4	164.1	163.8	164.1	164.4	164.1	163.8	164.1	164.4	164.1	163.9	164.1	164.4	164.1
σ^d (Valence Density)	3.0	35.1	40.0	26.0	3.0	36.5	38.1	25.9	2.5	36.5	38.1	25.7	2.7	36.7	37.6	25.7	6.6	34.9	36.0	25.8
σ^d	166.8	199.2	204.4	190.1	166.8	200.6	202.5	190.0	166.3	200.6	202.5	189.8	166.5	200.8	202.0	189.8	170.5	199.0	200.4	190.0
σ^p (OCC-OCC)	24.3	24.7	89.2	46.0	31.2	33.0	96.1	53.4	30.4	33.0	98.7	54.0	31.5	43.3	93.8	56.2	28.8	49.0	87.7	55.2
σ^p (OCC-VIR)	-200.6	-170.4	-161.8	-177.6	-220.7	-189.5	-168.4	-192.9	-226.0	-191.4	-165.4	-194.3	-219.1	-205.9	-167.4	-197.5	-227.9	-182.3	-166.8	-192.3
σ^p	-135.7	-132.7	-79.3	-115.9	-137.2	-133.2	-90.3	-120.2	-142.3	-129.0	-91.0	-120.7	-139.1	-131.4	-90.0	-120.2	-140.0	-134.1	-79.4	-117.8
Total	63.7	71.4	87.6	74.2	65.1	67.8	76.5	69.8	59.8	71.9	75.4	69.0	62.6	69.7	76.5	69.6	59.9	64.3	92.2	72.1

[a] Calculated boron magnetic shielding tensor components for each boronic acid and ester compound studied. Calculated values for boronic acid dimers which take into account hydrogen bonding interactions were used for **1** to **5**. ADF calculations were performed using the GGA revPBE functional and TZP basis set on all atoms.

Table S5. Calculated magnetic shielding tensor components for phenylboronic acid.[a]

Dihedral	0				10				20				30				40			
Contribution	σ_{11}	σ_{22}	σ_{33}	σ_{iso}	σ_{11}	σ_{22}	σ_{33}	σ_{iso}	σ_{11}	σ_{22}	σ_{33}	σ_{iso}	σ_{11}	σ_{22}	σ_{33}	σ_{iso}	σ_{11}	σ_{22}	σ_{33}	σ_{iso}
σ^d (Core Density)	163.9	164.2	164.2	164.1	163.9	164.2	164.3	164.1	163.9	164.2	164.3	164.1	163.9	164.2	164.3	164.1	163.9	164.2	164.3	164.1
σ^d (Valence Density)	3.4	33.1	39.2	25.2	3.7	33.2	39.2	25.3	4.5	33.4	39.0	25.6	5.8	33.8	38.6	26.1	7.3	34.3	38.1	26.6
σ^d	167.3	197.3	203.4	189.3	167.6	197.4	203.5	189.5	168.4	197.6	203.3	189.8	169.7	198.0	202.9	190.2	171.2	198.5	202.4	190.7
σ^p (OCC-OCC)	7.7	18.5	33.4	19.9	7.7	18.2	33.3	19.7	7.5	17.3	33.1	19.3	7.3	15.9	32.9	18.7	7.3	14.3	32.7	18.1
σ^p (OCC-VIR)	-154.7	-143.4	-129.5	-142.6	-154.7	-145.3	-128.1	-142.7	-154.4	-149.3	-125.3	-143.0	-153.9	-153.5	-122.6	-143.4	-157.2	-153.5	-120.5	-143.7
σ^p	-136.2	-135.7	-81.7	-117.9	-136.4	-136.4	-81.7	-118.2	-138.1	-137.0	-81.9	-119.0	-140.3	-137.9	-82.2	-120.1	-142.3	-139.0	-82.6	-121.3
Total	61.2	67.7	85.6	71.5	61.0	66.6	86.2	71.3	60.7	64.0	87.5	70.7	60.2	61.1	88.9	70.1	58.5	59.5	90.1	69.4

Dihedral	50				60				70				80				90			
Contribution	σ_{11}	σ_{22}	σ_{33}	σ_{iso}	σ_{11}	σ_{22}	σ_{33}	σ_{iso}	σ_{11}	σ_{22}	σ_{33}	σ_{iso}	σ_{11}	σ_{22}	σ_{33}	σ_{iso}	σ_{11}	σ_{22}	σ_{33}	σ_{iso}
σ^d (Core Density)	163.9	164.2	164.3	164.1	163.9	164.2	164.3	164.1	163.9	164.2	164.3	164.1	163.9	164.1	164.3	164.1	163.9	164.1	164.3	164.1
σ^d (Valence Density)	8.9	34.7	37.5	27.1	10.4	35.1	36.9	27.5	11.7	35.5	36.3	27.8	12.6	35.7	36.0	28.1	12.9	35.7	35.8	28.1
σ^d	172.8	198.9	201.8	191.2	174.3	199.3	201.2	191.6	175.6	199.7	200.6	191.9	176.5	199.8	200.3	192.2	176.8	199.8	200.1	192.3
σ^p (OCC-OCC)	7.3	12.6	32.5	17.5	7.4	11.1	32.4	17.0	7.5	10.0	32.3	16.6	7.6	9.3	32.2	16.4	7.7	9.1	32.2	16.3
σ^p (OCC-VIR)	-159.9	-153.1	-118.8	-143.9	-161.7	-152.8	-117.6	-144.0	-162.9	-152.7	-116.9	-144.1	-163.5	-152.6	-116.4	-144.2	-163.6	-152.6	-116.2	-144.2
σ^p	-143.7	-140.2	-83.0	-122.3	-144.6	-141.4	-83.4	-123.1	-145.0	-142.4	-83.6	-123.7	-145.2	-143.0	-83.8	-124.0	-145.2	-143.3	-83.8	-124.1
Total	56.7	58.8	91.0	68.8	55.6	58.0	91.8	68.5	55.0	57.4	92.4	68.3	54.8	56.9	92.8	68.2	54.8	56.7	93.0	68.2

[a] Calculated boron magnetic shielding tensor components for phenylboronic acid as ϕ_{CCBO} is varied from 0 to 90 degrees. ADF calculations were performed using the GGA revPBE functional and TZP basis set on all atoms.

Table S6. Calculated magnetic shielding tensor components and Ω for phenylboronic acid monomer and dimer as the dihedral is varied from 0 to 90º.[a]

	Monomer[b]				Dimer[b]			
ϕ_{CCBO} / º	σ_{11}	σ_{22}	σ_{33}	Ω / ppm	σ_{11}	σ_{22}	σ_{33}	Ω / ppm
0	61.2	67.7	85.6	24.4	56.9	72.5	83.0	26.1
10	61.0	66.6	86.2	25.2	56.2	71.9	83.7	27.5
20	60.7	64.0	87.5	26.8	54.8	69.9	85.3	30.5
30	60.2	61.0	88.9	28.7	53.1	67.6	86.8	33.7
40	58.5	59.5	90.1	31.6	51.5	65.5	88.1	36.6
50	56.7	58.8	91.0	34.3	50.4	63.7	89.2	38.8
60	55.6	58.0	91.8	36.2	49.8	62.2	90.3	40.5
70	55.0	57.4	92.4	37.4	49.7	60.9	91.2	41.5
80	54.8	56.9	92.8	38.0	49.9	59.9	91.9	42.0
90	54.8	56.7	93.0	38.2	50.3	29.2	92.3	42.0

	Monomer[c]				Dimer[c]			
ϕ_{CCBO} / º	σ_{11}	σ_{22}	σ_{33}	Ω / ppm	σ_{11}	σ_{22}	σ_{33}	Ω / ppm
0	80.1	80.1	97.8	17.7	73.3	87.9	96.1	22.8
10	79.8	80.0	98.1	18.3	72.7	87.5	96.8	24.1
20	79.1	79.9	98.7	19.6	71.3	86.1	98.3	27.0
30	78.2	79.6	99.6	21.4	69.7	84.6	99.9	30.2
40	77.3	79.3	100.5	23.2	68.3	83.1	101.2	32.9
50	76.5	78.9	101.4	24.9	67.3	81.8	102.3	35.0
60	75.7	78.6	102.5	26.8	66.9	80.4	103.4	36.5
70	74.9	78.2	103.8	28.9	66.8	79.2	104.4	37.6
80	74.1	77.7	105.3	31.2	67.0	78.1	105.0	38.0
90	73.1	77.1	106.9	33.8	67.5	77.2	105.3	37.8

[a] Calculated boron ϕ_{CCBO}, Ω, and shielding tensor components for phenylboronic acid monomer and dimer as ϕ_{CCBO} is varied from 0 to 90º.

[b] Hybrid DFT calculations were performed using the B3LYP functional and the 6-31G* basis set on all first and second row elements, while the aug-cc-pVTZ basis set was used on all heavier elements.

[c] ADF calculations were performed using the GGA revPBE functional and TZP basis set on all atoms.

Table S7. Calculated magnetic shielding tensor components with the largest contribution to total isotropic σ_{para} for a given set of occupied and virtual MOs for compounds **1** to **10**.[a]

Compound	MOs (OCC-VIR)	σ_{11}[b]	σ_{22}[b]	σ_{33}[b]	σ_{iso}	ΔE	ϕ_{CCBO} / °	Ω / ppm
1	102-201	0	0	-6	-2	0.4615	8.7	25.0
2	43-70	-2	-58	0	-20	0.3156	90.0	41.8
3	42-75	-8	-8	0	-5	0.4240	0.1	27.7
4	45-67	-6	0	-9	-5	0.3377	0.0	23.4
5	49-81	0	-12	0	-4	0.3887	19.9	28.1
6	33-65	0	-16	0	-5	0.4553	0.5	23.9
7	39-74	-17	0	0	-5	0.4379	3.0	11.5
8	39-59	-20	0	0	-7	0.3444	2.9	15.5
9	46-70	-12	0	0	-4	0.3389	1.2	14.0
10	43-60	0	-7	-5	-4	0.3290	61.3	32.3

[a] Calculated boron ϕ_{CCBO}, Ω, shielding tensor components, and energy gap for each pair of occupied and virtual orbitals which have the largest contribution to total isotropic σ_{para} for each boronic acid and ester compound studied. The shielding tensor components are those for the given pair of MOs, and are not the total shielding values. Calculated values for boronic acid dimers which take into account hydrogen bonding interactions are included where applicable. ADF calculations were performed using the GGA revPBE functional and TZP basis set on all atoms.

[b] Contributions (ppm) to shielding tensor principal components for a given pair of MOs which yield the largest contribution to total isotropic paramagnetic shielding.

Table S8. Calculated magnetic shielding tensor components with the largest contribution to total isotropic σ_{para} for a given set of occupied and virtual MOs for phenylboronic acid.[a]

Dihedral	MOs (OCC-VIR)	σ_{11}[b]	σ_{22}[b]	σ_{33}[b]	σ_{iso}	ΔE	Ω / ppm
0	21-36	0	-45	0	-15	0.4316	24.39
10	21-36	0	-38	-1	-13	0.4285	25.71
20	21-36	0	-27	-3	-9	0.4215	26.80
30	21-36	0	-18	-3	-7	0.4139	28.69
40	18-58	0	-12	-7	-6	0.6885	31.56
50	9-27	-19	0	0	-6	0.5202	34.33
60	9-27	-26	0	0	-9	0.5165	36.22
70	9-27	-32	0	0	-11	0.5127	37.39
80	9-27	0	-36	0	-12	0.5098	38.01
90	9-27	0	-38	0	-13	0.5087	38.20

[a] Calculated boron ϕ_{CCBO}, Ω, and shielding tensor components and energy gap for each pair of occupied and virtual orbitals which have the largest contribution to total isotropic paramagnetic shielding for phenylboronic acid as the dihedral is varied from 0 to 90 degrees. ADF calculations were performed using the GGA revPBE functional and TZP basis set on all atoms.

[b] Contributions (ppm) to shielding tensor principal components for a given pair of MOs which yield the largest contribution to total isotropic paramagnetic shielding.

Table S9. Calculated Ω and magnetic shielding tensor components for a series of steric, electron donating, and electron withdrawing groups substituted on phenylboronic acid.[a]

Compound[b]	σ_{11}[d]	σ_{22}[d]	σ_{33}[d]	Total σ_{para}	σ_{11}	σ_{22}	σ_{33}	Total σ_{iso}	Ω / ppm
phenylboronic acid	-136.2	-135.7	-81.7	-117.9	61.2	67.7	85.6	71.5	24.4
o-steric	-138.9	-132.2	-81.5	-117.5	58.7	72.4	85.4	72.2	26.7
m-steric	-136.3	-134.4	-80.9	-117.2	60.4	69.8	85.8	72.0	25.4
p-steric	-136.8	-134.4	-81.2	-117.5	61.0	68.8	85.7	71.8	24.7
mild o-EWG	-140.2	-138.4	-83.2	-120.6	56.1	58.3	93.9	69.4	37.9
mild m-EWG	-137.1	-133.4	-81.3	-117.3	60.1	70.1	85.3	71.8	25.3
mild p-EWG	-137.9	-132.7	-81.6	-117.4	59.7	70.5	85.4	71.9	25.7
strong o-EWG	-140.4	-133.7	-83.9	-119.3	56.4	63.2	92.6	70.7	36.2
strong m-EWG	-139.6	-132.5	-95.6	-122.6	55.3	60.1	92.8	69.4	37.5
strong p-EWG	-144.8	-140.7	-83.2	-122.9	55.3	58.7	93.1	69.1	37.8
mild o-EDG	-136.0	-133.4	-80.6	-116.7	59.5	70.5	86.4	72.2	27.0
mild m-EDG	-135.9	-133.6	-81.8	-117.1	59.9	70.3	85.8	72.0	25.8
mild p-EDG	-136.6	-133.1	-81.9	-117.2	60.7	69.8	85.6	72.0	24.9
strong o-EDG	-140.7	-132.4	-82.9	-118.7	61.4	66.1	84.6	70.7	23.2
strong m-EDG	-136.8	-135.3	-81.3	-117.8	61.9	66.8	85.7	71.4	23.7
strong p-EDG	-137.8	-133.8	-81.6	-117.7	63.9	65.7	85.6	71.8	21.7

Compound[c]	σ_{11}[d]	σ_{22}[d]	σ_{33}[d]	Total σ_{para}	σ_{11}	σ_{22}	σ_{33}	Total σ_{iso}	Ω / ppm
phenylboronic acid	-136.2	-135.7	-81.7	-117.9	61.2	67.7	85.6	71.5	24.4
o-steric	-137.8	-134.1	-81.6	-117.8	58.9	71.6	84.9	71.8	26.1
m-steric	-136.6	-134.8	-81.1	-117.5	60.5	69.0	85.6	71.7	25.1
p-steric	-136.7	-134.8	-81.3	-117.6	61.2	68.2	85.5	71.6	24.4
mild o-EWG	-136.5	-135.4	-81.3	-117.7	59.5	70.2	85.6	71.8	26.0
mild m-EWG	-137.1	-133.8	-81.4	-117.4	60.2	69.4	85.1	71.6	25.0
mild p-EWG	-137.9	-133.1	-81.7	-117.6	59.8	69.8	85.2	71.6	25.4
strong o-EWG	-137.2	-133.9	-80.1	-117.1	58.5	71.9	86.7	72.4	28.2
strong m-EWG	-136.8	-133.9	-81.0	-117.3	59.6	70.2	85.7	71.8	26.0
strong p-EWG	-137.8	-132.6	-81.3	-117.2	59.9	70.3	85.6	71.9	25.6
mild o-EDG	-134.8	-133.9	-81.8	-116.8	59.7	70.3	85.7	71.9	26.0
mild m-EDG	-136.1	-134.0	-82.0	-117.4	60.0	69.5	85.6	71.7	25.6
mild p-EDG	-136.4	-133.5	-82.1	-117.3	60.8	69.2	85.4	71.8	24.6
strong o-EDG	-140.9	-132.2	-82.1	-118.4	61.9	66.3	84.5	70.9	22.7
strong m-EDG	-136.3	-135.2	-81.3	-117.6	61.2	67.8	85.5	71.5	24.3
strong p-EDG	-135.9	-135.5	-81.8	-117.7	61.7	67.7	85.3	71.6	23.6

[a] Calculated boron Ω and magnetic shielding tensor components for substituted phenylboronic acid. ADF calculations were performed using the GGA revPBE functional and TZP basis set on all atoms. Bromine was used as a steric group, carboxyl as a mild electron withdrawing group, nitro as a strong electron withdrawing group, carboxylic acid ester as a mild electron donating group, and amine as a strong electron donating group.[b] Phenylboronic acid structure has been fully optimized. [c] Phenylboronic acid structure has ϕ_{CCBO} fixed at 0 degrees. [d] Shielding tensor component which contributes to total isotropic paramagnetic shielding.

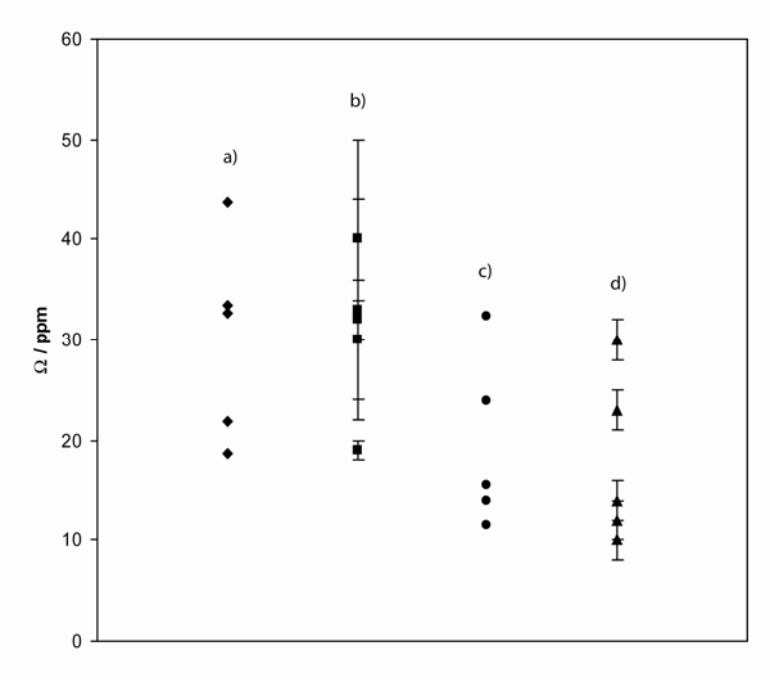

Figure S1. Calculated and experimental boron Ω values for boronic acids and boronic esters studied. Calculated values for boronic acid dimers which take into account hydrogen bonding interactions are included where applicable. ADF calculations were performed using the GGA revPBE functional and TZP basis set on all atoms. The following data are shown: a) calculated Ω values for boronic acids, b) experimental Ω values for boronic acids, c) calculated Ω values for boronic esters, and d) experimental Ω values for boronic esters.

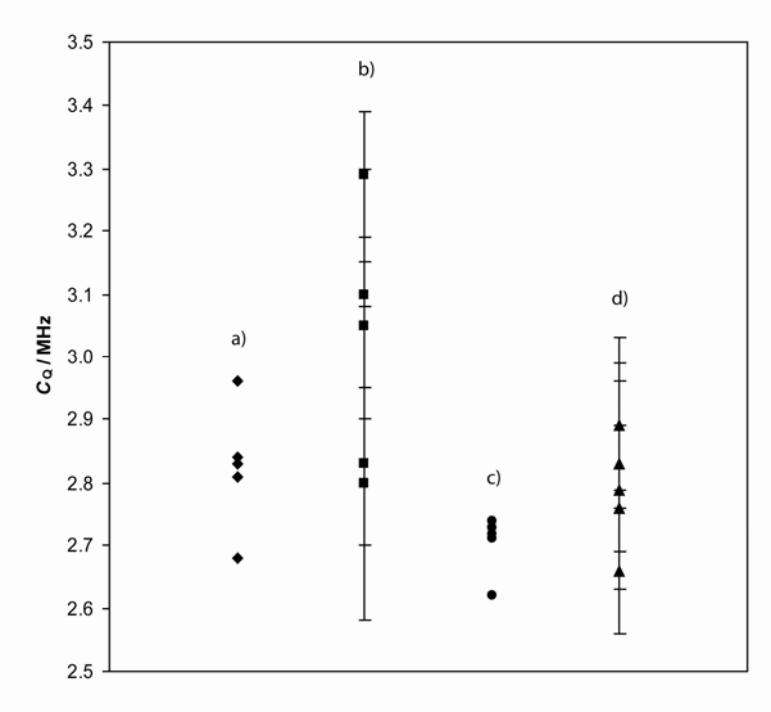

Figure S2. Calculated and experimental boron C_Q for boronic acids and boronic esters studied. Calculated values for boronic acid dimers which take into account hydrogen bonding interactions are included where applicable. ADF calculations were performed using the GGA revPBE functional and TZP basis set on all atoms. The following data are shown: a) calculated C_Q for boronic acids, b) experimental C_Q for boronic acids, c) calculated C_Q for boronic esters, and d) experimental C_Q for boronic esters.

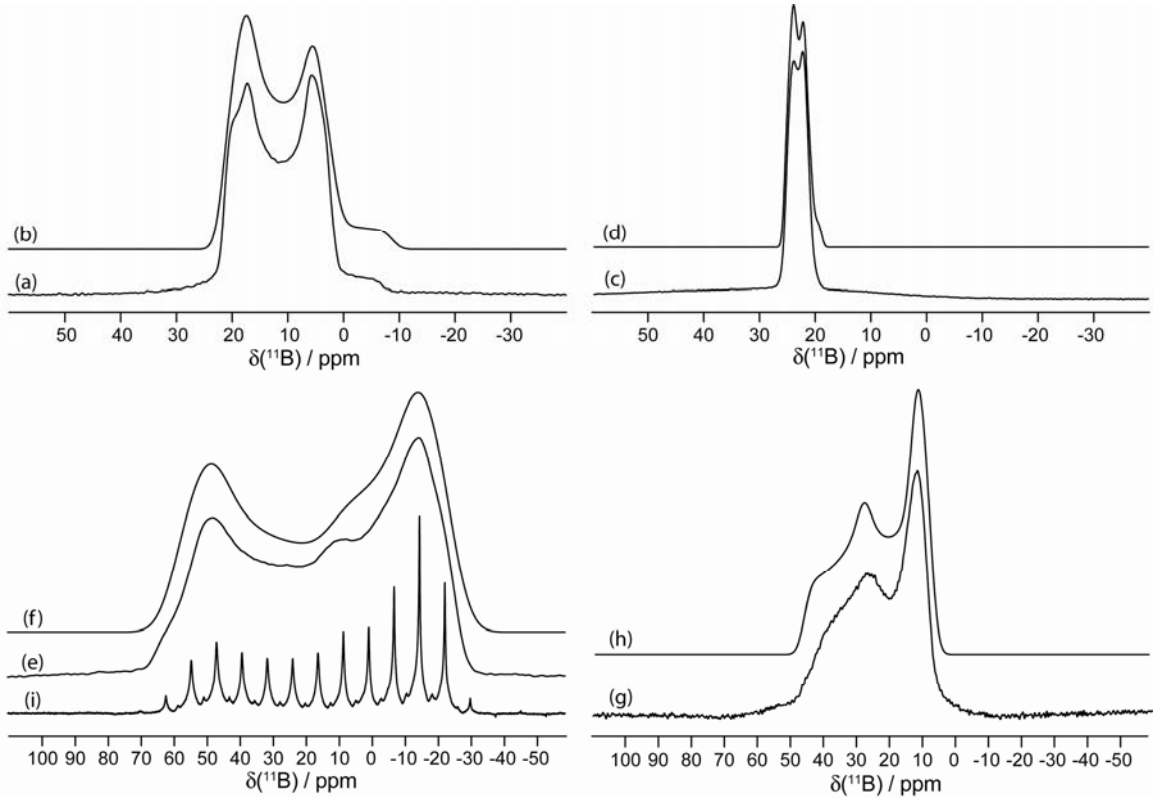

Figure S3. Solid-state boron-11 NMR spectroscopy of **5**. Experimental spectra of a powdered sample undergoing MAS are shown in (a) ^{11}B at 9.40 T and (c) ^{11}B at 21.1 T. Best-fit spectra were simulated using WSolids (traces (b) and (d)) using the parameters given in Table 1. Experimental spectra of stationary powdered samples are shown in (e) ^{11}B at 9.40 T and (g) ^{11}B at 21.1 T. Best-fit spectra were simulated using WSolids (traces (f) and (h)) using the parameters given in Table 1. Experimental QCPMG spectrum of a stationary powdered sample is shown in (i) ^{11}B at 9.40 T.

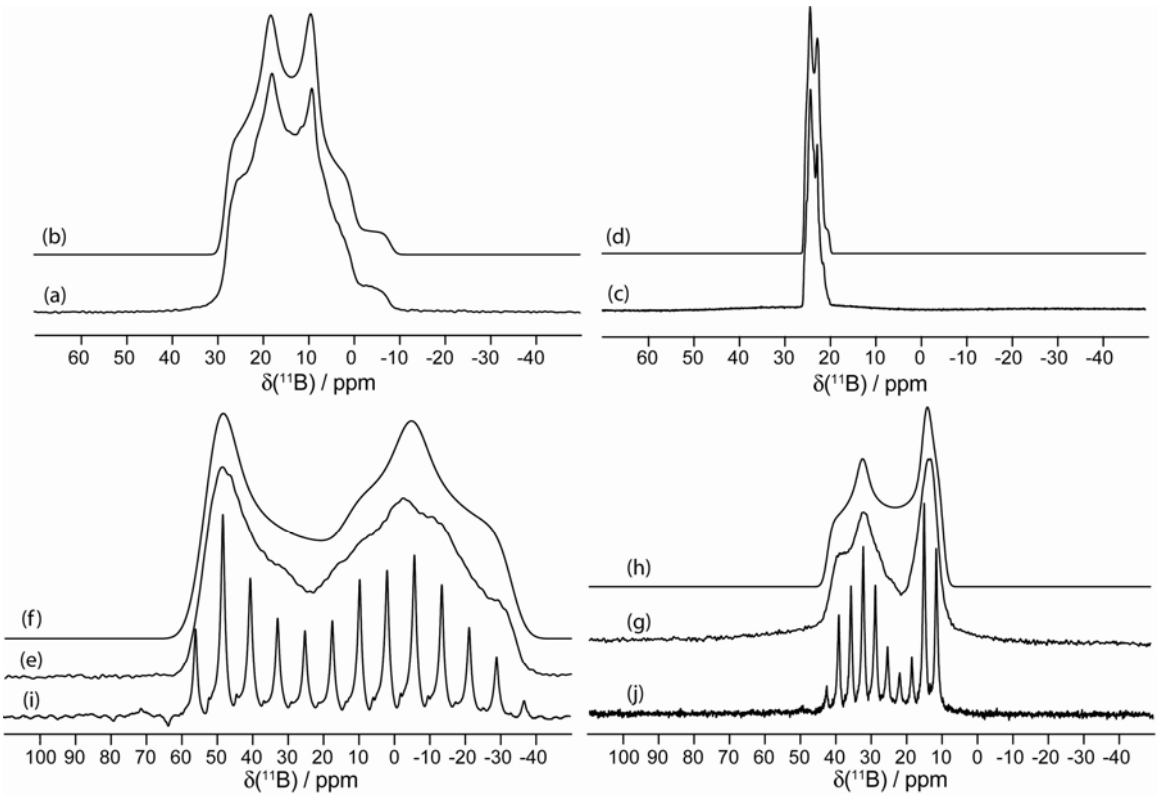

Figure S4. Solid-state boron-11 NMR spectroscopy of **6**. Experimental spectra of a powdered sample undergoing MAS are shown in (a) ^{11}B at 9.40 T and (c) ^{11}B at 21.1 T. Best-fit spectra were simulated using WSolids (traces (b) and (d)) using the parameters given in Table 1. Experimental spectra of stationary powdered samples are shown in (e) ^{11}B at 9.40 T and (g) ^{11}B at 21.1 T. Best-fit spectra were simulated using WSolids (traces (f) and (h)) using the parameters given in Table 1. Experimental QCPMG spectra of stationary powdered samples are shown in (i) ^{11}B at 9.40 T and (j) ^{11}B at 21.1 T.

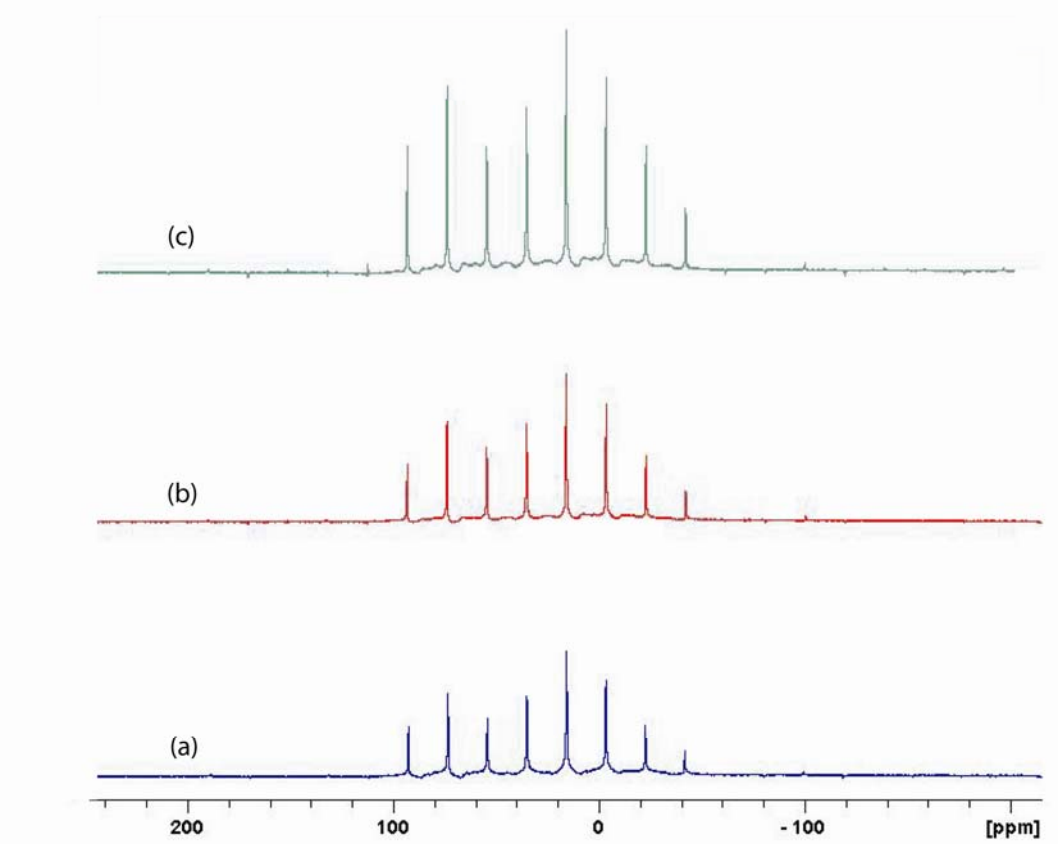

Figure S5. Solid-state boron NMR spectroscopy of **1**. Experimental ^{11}B spectra of stationary powdered samples at 9.40 T are shown in (a) using the QCPMG pulse sequence, (b) using the modified-QCPMG pulse sequence with a signal enhancement factor of 1.18, and (c) using the DFS modified-QCPMG pulse sequence with a signal enhancement factor of 1.96 relative to QCPMG. Spikelets are separated by 2500 Hz.

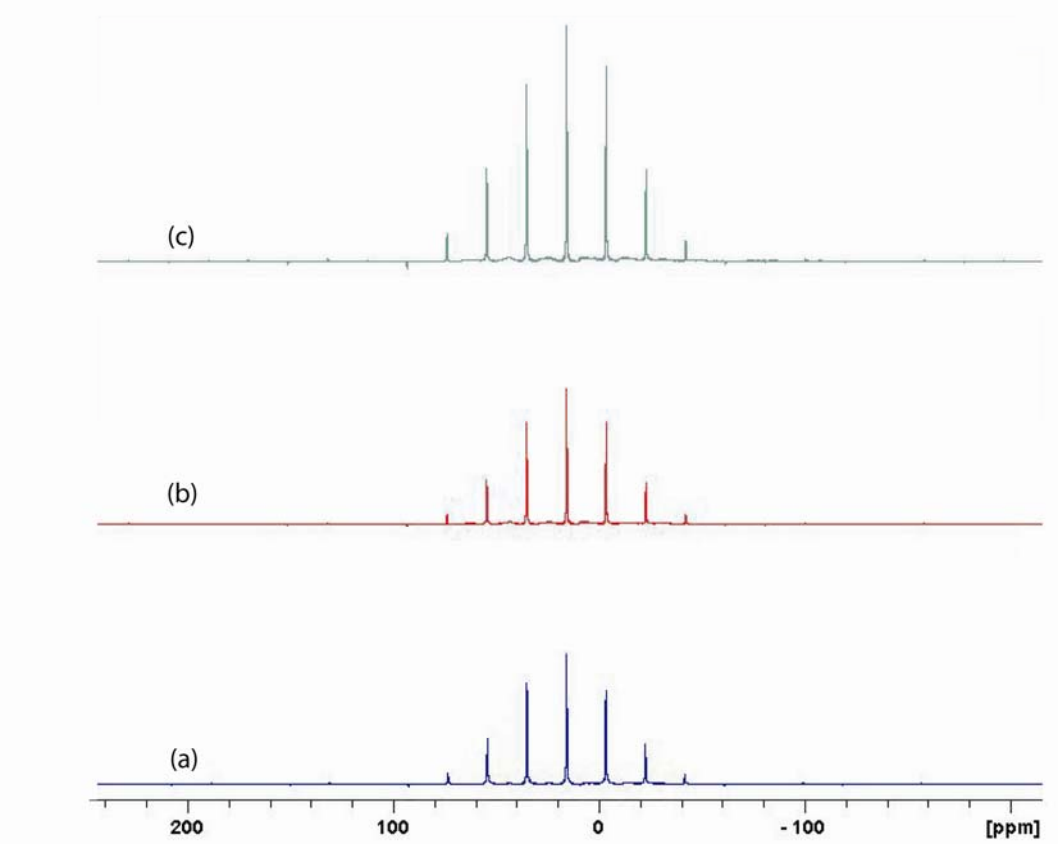

Figure S6. Solid-state boron NMR spectroscopy of **2**. Experimental ^{11}B spectra of stationary powdered samples at 9.40 T are shown in (a) using the QCPMG pulse sequence, (b) using the modified-QCPMG pulse sequence with a signal enhancement factor of 1.05, and (c) using the DFS modified-QCPMG pulse sequence with a signal enhancement factor of 1.85 relative to QCPMG. Spikelets are separated by 2500 Hz.

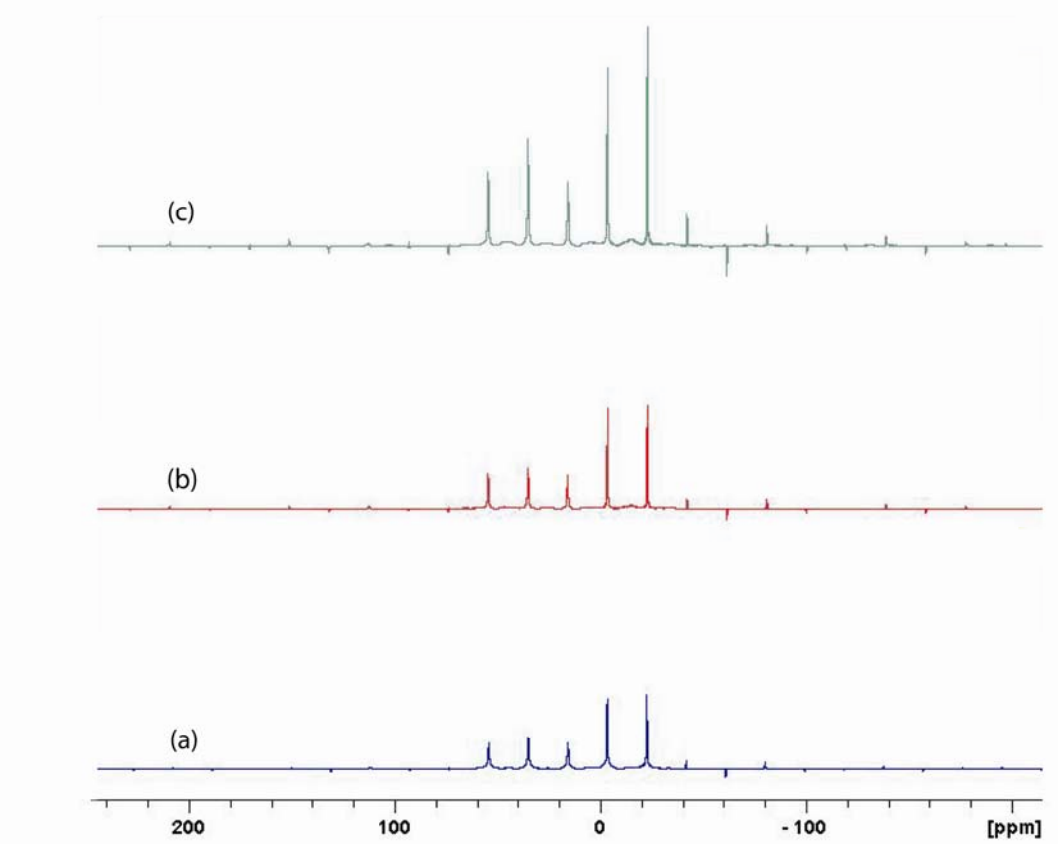

Figure S7. Solid-state boron NMR spectroscopy of **5**. Experimental ^{11}B spectra of stationary powdered samples at 9.40 T are shown in (a) using the QCPMG pulse sequence, (b) using the modified-QCPMG pulse sequence with a signal enhancement factor of 1.42, and (c) using the DFS modified-QCPMG pulse sequence with a signal enhancement factor of 2.95 relative to QCPMG. Spikelets are separated by 2500 Hz.

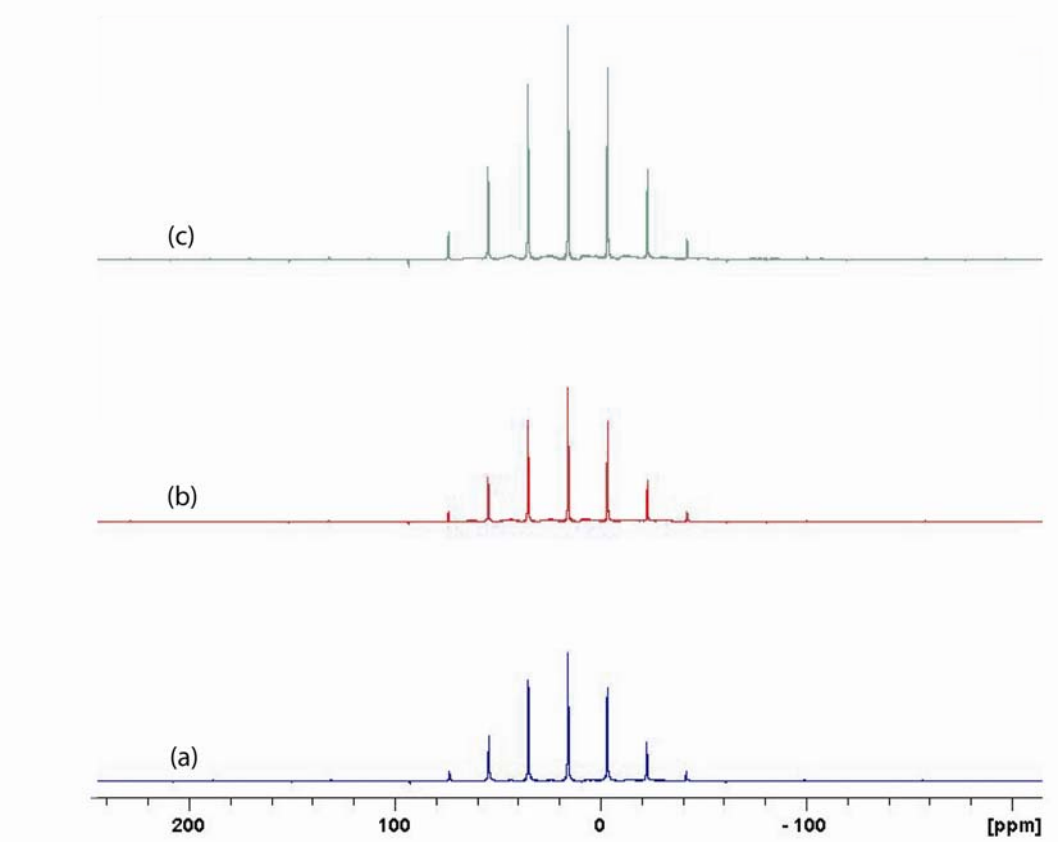

Figure S8. Solid-state boron NMR spectroscopy of **8**. Experimental ^{11}B spectra of stationary powdered samples at 9.40 T are shown in (a) using the QCPMG pulse sequence, (b) using the modified-QCPMG pulse sequence with a signal enhancement factor of 1.05, and (c) using the DFS modified-QCPMG pulse sequence with a signal enhancement factor of 1.80 relative to QCPMG. Spikelets are separated by 2500 Hz.

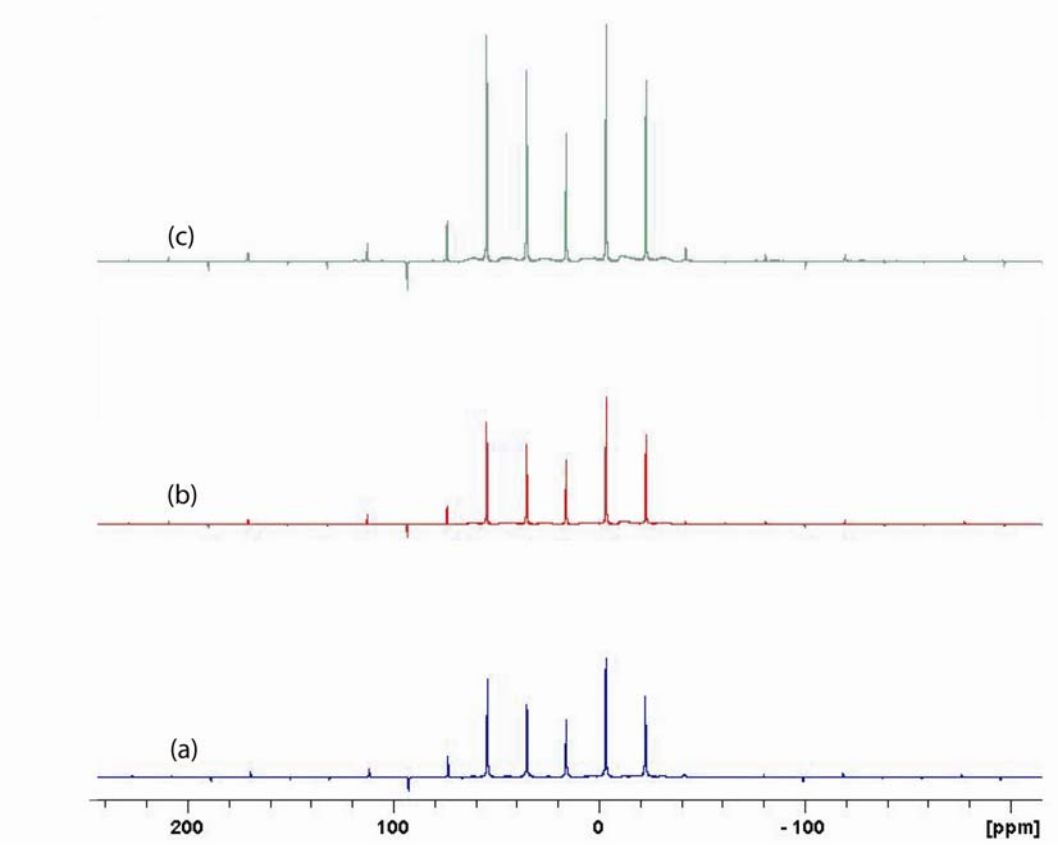

Figure S9. Solid-state boron NMR spectroscopy of **10**. Experimental ^{11}B spectra of stationary powdered samples at 9.40 T are shown in (a) using the QCPMG pulse sequence, (b) using the modified-QCPMG pulse sequence with a signal enhancement factor of 1.09, and (c) using the DFS modified-QCPMG pulse sequence with a signal enhancement factor of 2.04 relative to QCPMG. Spikelets are separated by 2500 Hz.

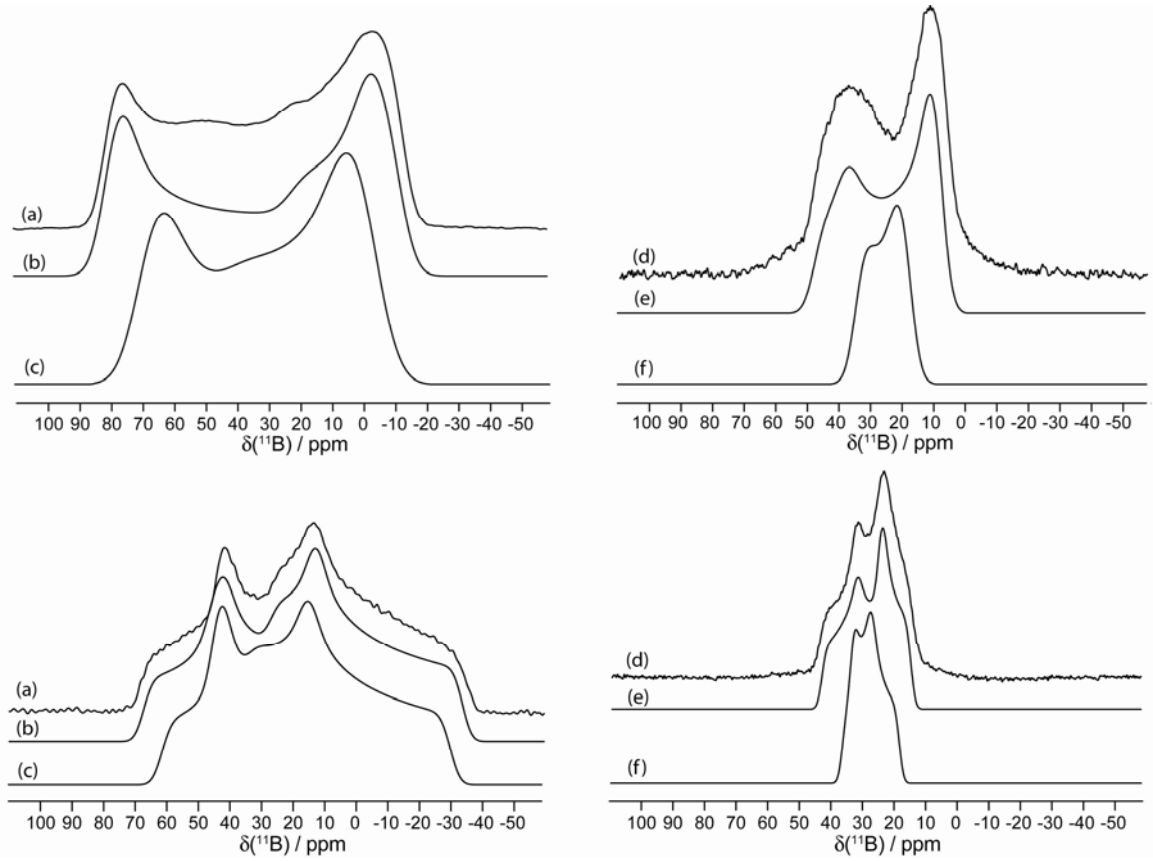

Figure S10. Solid-state boron-11 NMR spectroscopy of **3** (top), and **8** (bottom). Experimental spectra of stationary powdered samples are shown in (a) ^{11}B at 9.40 T and (d) ^{11}B at 21.1 T. Best-fit spectra were simulated using WSolids (traces (b) and (e)) using the parameters given in Table 1. Best-fit spectra not taking the effects of CSA into account were simulated using WSolids (traces (c) and (f)) using the parameters given in Table 1, but where the values for span were set to 0 ppm.

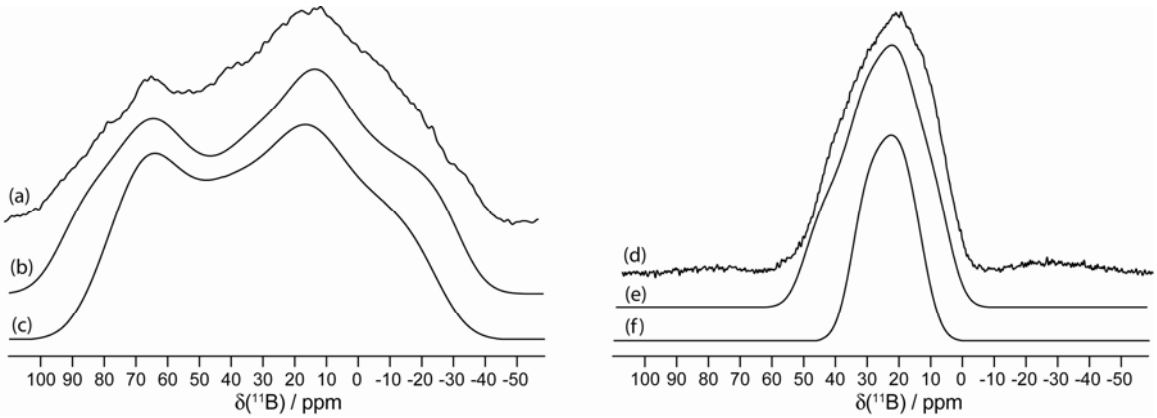

Figure S11. Solid-state boron-11 NMR spectroscopy of **1**. Experimental spectra of stationary powdered samples are shown in (a) ^{11}B at 9.40 T and (d) ^{11}B at 21.1 T. Best-fit spectra were simulated using WSolids (traces (b) and (e)) using the parameters given in Table 1. Best-fit spectra not taking the effects of CSA into account were simulated using WSolids (traces (c) and (f)) using the parameters given in Table 1, but where the values for Ω were set to 0 ppm.

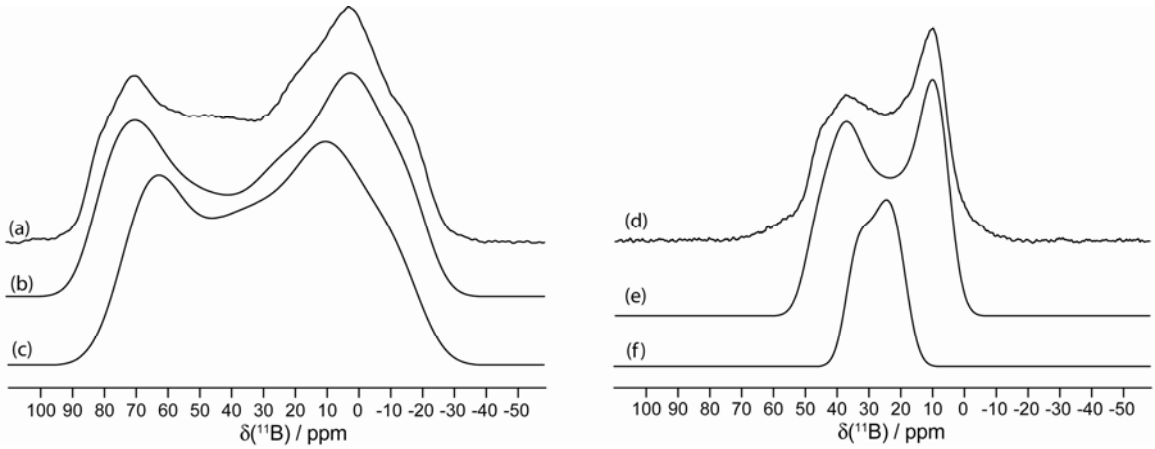

Figure S12. Solid-state boron-11 NMR spectroscopy of **2**. Experimental spectra of stationary powdered samples are shown in (a) ^{11}B at 9.40 T and (d) ^{11}B at 21.1 T. Best-fit spectra were simulated using WSolids (traces (b) and (e)) using the parameters given in Table 1. Best-fit spectra not taking the effects of CSA into account were simulated using WSolids (traces (c) and (f)) using the parameters given in Table 1, but where the values for Ω were set to 0 ppm.

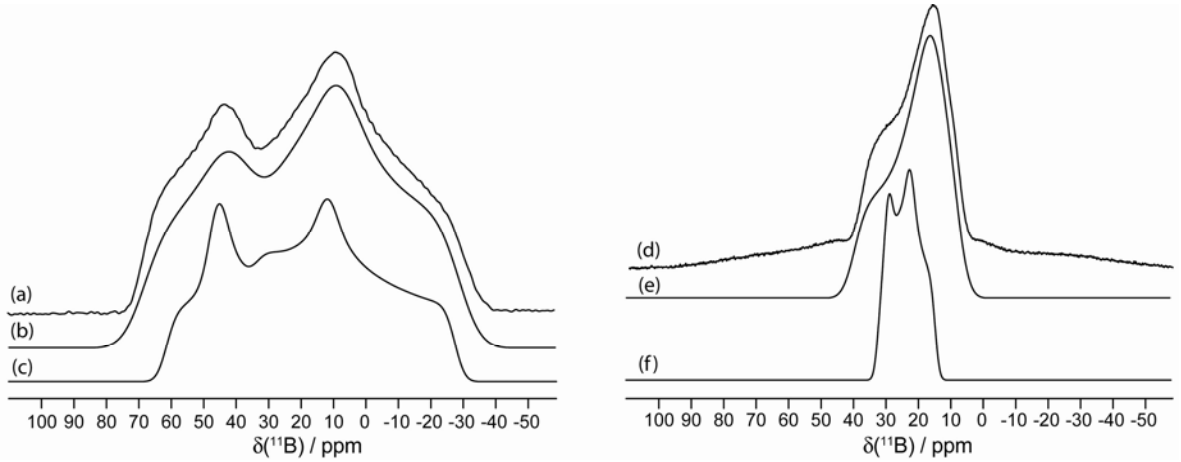

Figure S13. Solid-state boron-11 NMR spectroscopy of **4**. Experimental spectra of stationary powdered samples are shown in (a) ^{11}B at 9.40 T and (d) ^{11}B at 21.1 T. Best-fit spectra were simulated using WSolids (traces (b) and (e)) using the parameters given in Table 1. Best-fit spectra not taking the effects of CSA into account were simulated using WSolids (traces (c) and (f)) using the parameters given in Table 1, but where the values for Ω were set to 0 ppm.

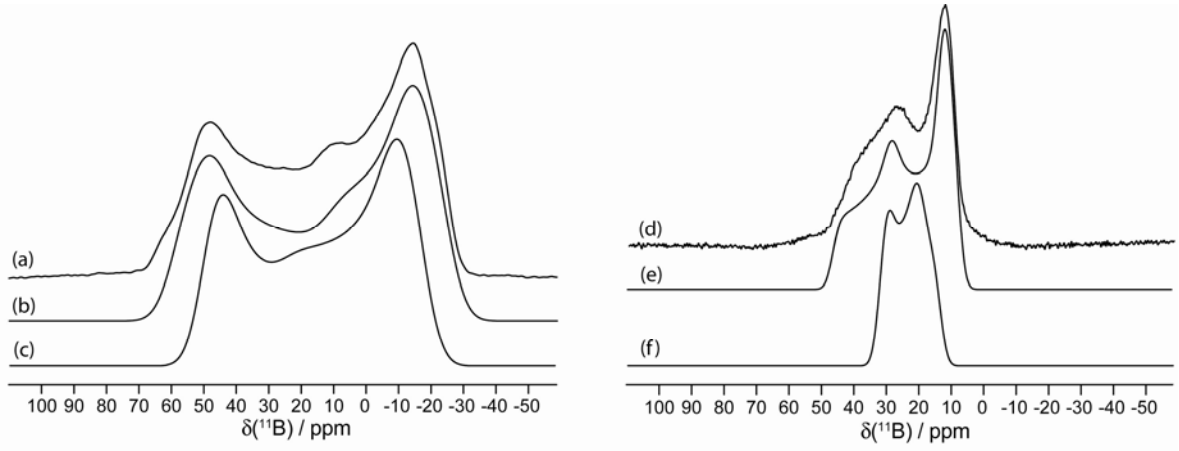

Figure S14. Solid-state boron-11 NMR spectroscopy of **5**. Experimental spectra of stationary powdered samples are shown in (a) ^{11}B at 9.40 T and (d) ^{11}B at 21.1 T. Best-fit spectra were simulated using WSolids (traces (b) and (e)) using the parameters given in Table 1. Best-fit spectra not taking the effects of CSA into account were simulated using WSolids (traces (c) and (f)) using the parameters given in Table 1, but where the values for Ω were set to 0 ppm.

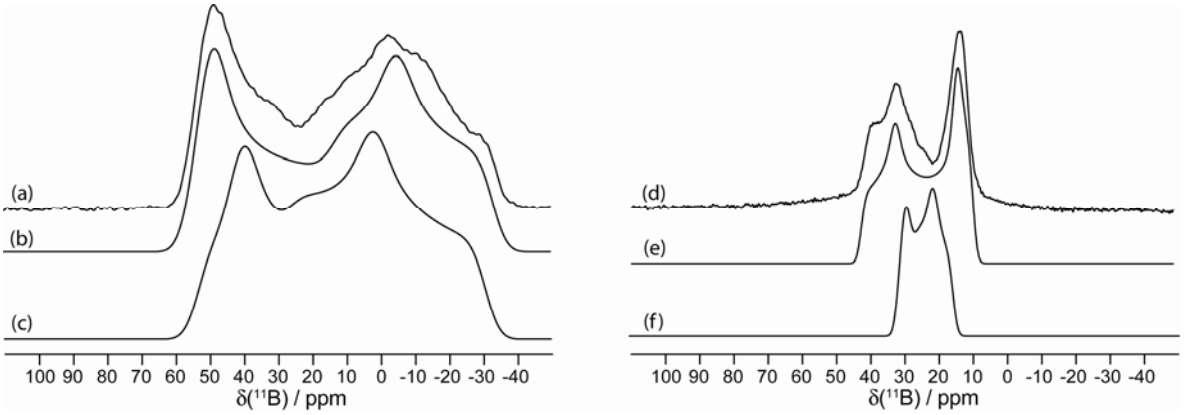

Figure S15. Solid-state boron-11 NMR spectroscopy of **6**. Experimental spectra of stationary powdered samples are shown in (a) ^{11}B at 9.40 T and (d) ^{11}B at 21.1 T. Best-fit spectra were simulated using WSolids (traces (b) and (e)) using the parameters given in Table 1. Best-fit spectra not taking the effects of CSA into account were simulated using WSolids (traces (c) and (f)) using the parameters given in Table 1, but where the values for Ω were set to 0 ppm.

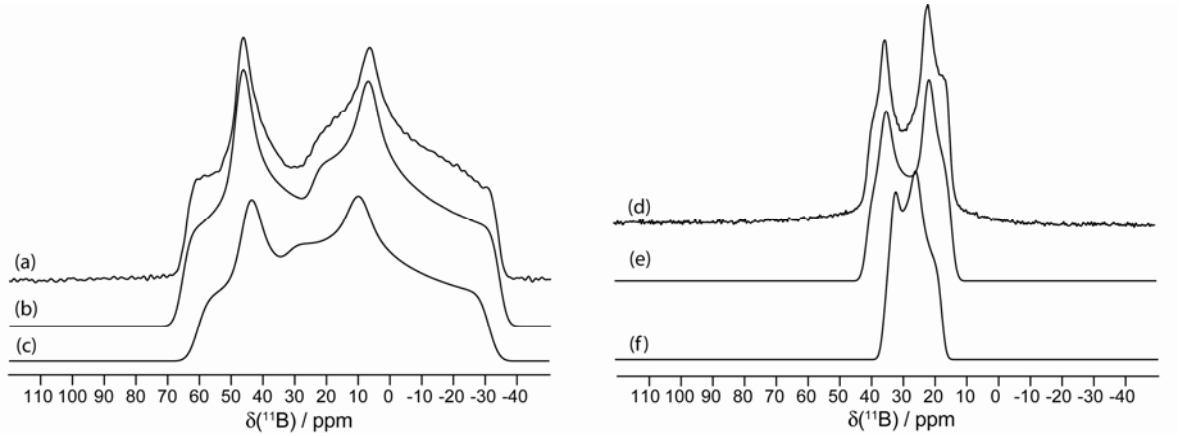

Figure S16. Solid-state boron-11 NMR spectroscopy of **7**. Experimental spectra of stationary powdered samples are shown in (a) ^{11}B at 9.40 T and (d) ^{11}B at 21.1 T. Best-fit spectra were simulated using WSolids (traces (b) and (e)) using the parameters given in Table 1. Best-fit spectra not taking the effects of CSA into account were simulated using WSolids (traces (c) and (f)) using the parameters given in Table 1, but where the values for Ω were set to 0 ppm.

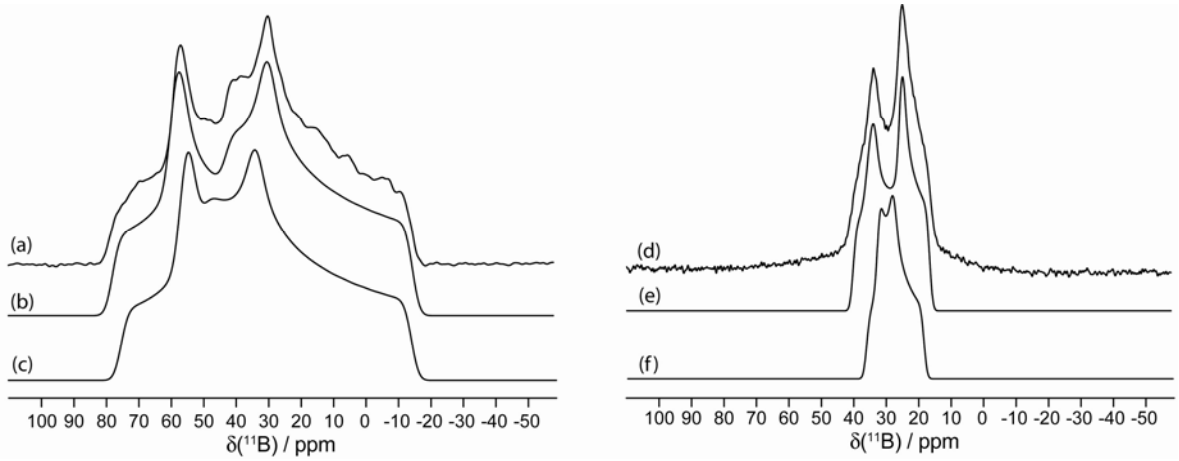

Figure S17. Solid-state boron-11 NMR spectroscopy of **9**. Experimental spectra of stationary powdered samples are shown in (a) ^{11}B at 9.40 T and (d) ^{11}B at 21.1 T. Best-fit spectra were simulated using WSolids (traces (b) and (e)) using the parameters given in Table 1. Best-fit spectra not taking the effects of CSA into account were simulated using WSolids (traces (c) and (f)) using the parameters given in Table 1, but where the values for Ω were set to 0 ppm.

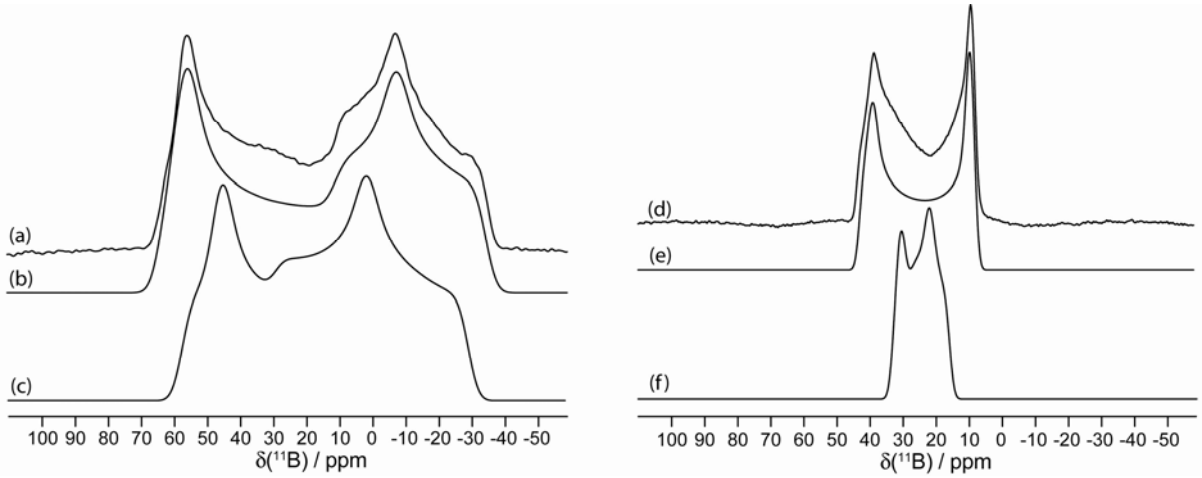

Figure S18. Solid-state boron-11 NMR spectroscopy of **10**. Experimental spectra of stationary powdered samples are shown in (a) ^{11}B at 9.40 T and (d) ^{11}B at 21.1 T. Best-fit spectra were simulated using WSolids (traces (b) and (e)) using the parameters given in Table 1. Best-fit spectra not taking the effects of CSA into account were simulated using WSolids (traces (c) and (f)) using the parameters given in Table 1, but where the values for Ω were set to 0 ppm.